SECOND EUROPEAN CONFERENCE ON EARTHQUAKE ENGINEERING
AND SEISMOLOGY, ISTANBUL AUG. 25-29, 2014

DYNAMIC RUPTURE SCENARIOS ON A FAULT NETWORK: THE CORINTH RIFT CASE

Virginie DURAND[1], Sébastien HOK[2], Aurélien BOISELET[3], Pascal BERNARD[4] and Oona SCOTTI[5]

In this work, we develop an original approach at the interface between physically-based earthquake rupture modelling and the need of earthquake scenario definition for seismic hazard assessment purposes.

We are investigating the seismic hazard of the Corinth rift region (Greece). Seismic hazard assessment needs an estimation of the maximum magnitude to be expected in a given area. Given the geometry of known faults of the region, characteristic earthquake magnitude can be evaluated using scaling laws (e.g. Leonard, 2010). However, historical seismicity and paleoseismological investigations indicate that larger earthquakes may occur. Those large earthquakes may require several faults to interact and break simultaneously, producing multiple segment ruptures.

In order to evaluate the multi-segment rupture (and associated magnitudes) feasibility, we compute the rupture propagation along the faults using a dynamic approach, using the numerical code developed by Hok and Fukuyama (2011). Dynamic rupture computation allows to use mechanical parameters (stress, fault geometry, friction) as inputs to get the macroscopic parameters of earthquakes (magnitude, slip, rupture velocities, rupture length, etc.) without *a priori*, but resulting from the spontaneous rupture propagation. It also allows to model the complexity of the fault network and to use robust observations such as long-term deformation as a constraint on the earthquake scenarios.

We focus our work on the south-western side of the rift, from the fault of Psathopyrgos to the fault of Aigion. The parameters of the models are: the geometry of the faults, the stress field acting on the faults, the position in the earthquake cycle, the frictional behaviour of the faults, and the location of the initiation of the rupture. The characteristics of the scenarios we are looking at are: the magnitude of the earthquake, its average slip, and the length of the rupture (the number of segments ruptured). The exploration of the different model parameters is done following a logic tree, so that one can analyze their impact on the variability of the resulting scenarios of earthquakes. In this way one can propagate the model parameter uncertainties on the variability of the obtained scenarios, which can facilitate their integration in a PSHA framework.

The modelled fault network is composed of a couple of subparallel faults (Psathopyrgos fault and Aigion fault) that are parallel to the shoreline of the gulf, linked by an oblique structure that connects the two faults (so-called Neos-Erineos). In order to investigate the influence of the fault geometries, we test 2 cases which differ regarding the intermediate oblique structure: in the first it is considered as a single fault plane, while in the second it is divided into 3 small segments following the surface mapping (Figure 1; Lambiri, Selianitika and Fassouleika faults). All faults have a dip angle of 60 degrees. Maximum depth of these faults is 7km, consistently with seismological data.

1 Dr, IPGP, Paris, vdurand@ipgp.fr
2 Dr, IRSN, Fontenay-Aux-Roses, sebastien.hok@irsn.fr
3 Dr, ENS-IRSN, Paris-Fontenay-Aux-Roses, boiselet@geologie.ens.fr
4 Dr, IPGP, Paris, bernard@ipgp.fr
5 Dr, IRSN, Fontenay-Aux-Roses, oona.scotti@irsn.fr

The stress field applied on the faults is depth-dependent. The vertical principal stress σ1 is equal to the lithostatic pressure, and horizontal components σ2 and σ3 are a linear function of the vertical stress value. σ3 value is assumed to be 1/3 of σ1, while its direction is chosen to be consistent with geodetic measurements showing that the extension is N10. We considered σ2=σ1, in order to be consistent with observed transtensional motion such as the 2001 earthquake (Pacchiani and Lyon-Caen, 2010). The stress field is not changed between the different scenarios.

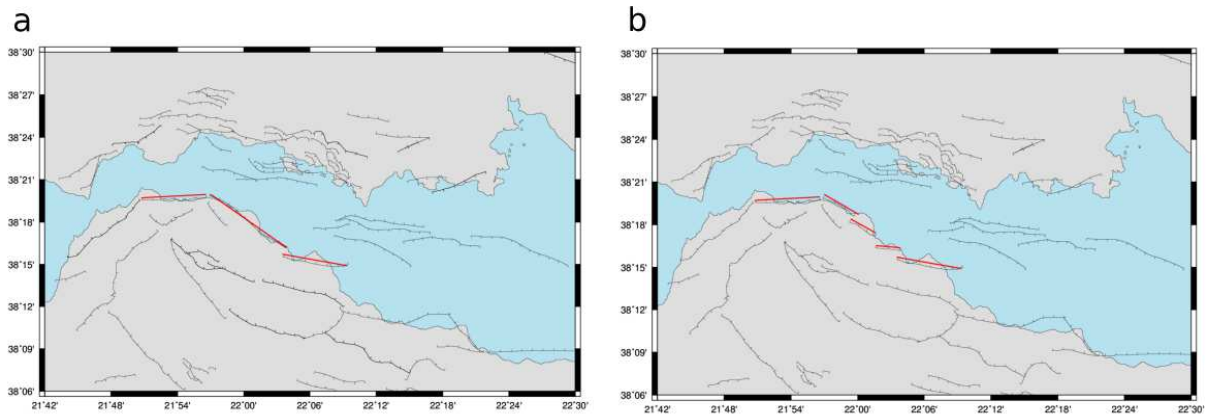

Figure 1. The fault geometries used in our simulations are indicated by the red lines. a) Simple geometry, with three segments, b) Complex geometry, with five segments. (Faults in black are courtesy of N.Meyer).

One of the parameters that we modify is the position in the seismic cycle for each fault segment. Using historical data, we assume an average recurrence time for a given fault (Boiselet, 2014), and knowing the date of the last earthquake, we can estimate roughly where the fault is in its cycle. We defined c as a parameter ranging from 0 just after an earthquake up to 1 just before the earthquake. Given uncertainties on the c value we tested 2 values for each fault segment. The implementation of c is done inside the friction law, as detailed in the following.

The earthquake rupture process is computed assuming a constitutive relation linking the stress acting on a fault element and the dislocation at each time. The fault is locked until the friction (ratio of shear to normal stress) exceeds a certain threshold (see Figure 2). This static value of friction is set to 0.6, at maximum, when c=0. However, if c>0, the static coefficient of friction is lowered down to the value of the applied initial friction (ratio of initial shear stress to the initial normal stress) when c=1. The fault is easier to break at the end of its cycle than just after an earthquake. For each scenario, we set a unique value of c at each fault; therefore each fault has a unique value of static friction.

To initiate the rupture, a circular area of the fault is set to have a value of static friction slightly below the initial value of friction. In our scenarios, we tested 2 different areas of initiation (one on each side of the fault network). To compute the spontaneous rupture propagation, at each fault element and at each time, the constitutive relation is solved. When the fault slips, the shear stress drops. The friction is set to evolve as a slip-weakening law (Figure 2 right inset). The slip-weakening law has 2 parameters (the static friction being fixed as previously explained), a value of dynamic friction associated to a critical slip distance Dc. The value of friction is linearly interpolated between the static and dynamic value, between 0 and Dc. When slip is larger than Dc, the friction remains constant and equal to the dynamic friction. In our modelling we obtain the dynamic friction coefficient by prescribing the stress drop value (difference between initial stress and final stress) $\Delta\sigma$ to 4 MPa, between 2 and 7 km depth. Fault areas shallower than 2 km have a lower stress drop (down to 0 MPa stress drop at the surface). The stress drop, hence the dynamic friction coefficients, are depth-dependent but not fault-dependent; they are identical between the different scenarios. The critical slip distance Dc is varied between the scenarios. Values tested are 0.1, 0.2, 0.3 and 0.4 meters. The value of Dc is kept the same on all the faults inside one given computation.

Our results (64 simulations) show different rupture scenarios depending on the parameter values. In the case of the simplest geometry (three faults), for a given area of initiation, we see two different behaviors, depending on the value of Dc. Either the rupture is stopped on the first fault (Figure 2a), either it propagates on all the three faults. In the case of the more complex geometry (five faults), we observe more variability, also depending on the value of Dc: either the rupture stays on the first fault, either it propagates on two faults, either on the five faults (Figure 2b). Each type of scenario (a given number of ruptured segments) can be obtained with both locations for the nucleation area. The maximum magnitude we obtain, when all the faults are broken, is Mw 6.4.

The maximum magnitude we obtained so far seems small compared to historical and paleoseismological studies, from which a minimal value for Mmax of 6.6 can be inferred. However, in our scenarios, we did not consider possible connection at depth between the faults (there is a gap), and we used only shallow faults. The gulf has also deeper seismogenic blind faults (e.g. 1995 Ms6.2 Aigion earthquake) that, if broken together with surface faults, could help to increase the magnitude.

In addition, we are currently testing other parameters, like the friction threshold and the stress drop, to achieve more dependence on the position in the seismic cycle and more variability in the scenarios - for example a two-segment rupture in the simple geometry case, or a three-segment rupture in the case of the complex geometry.

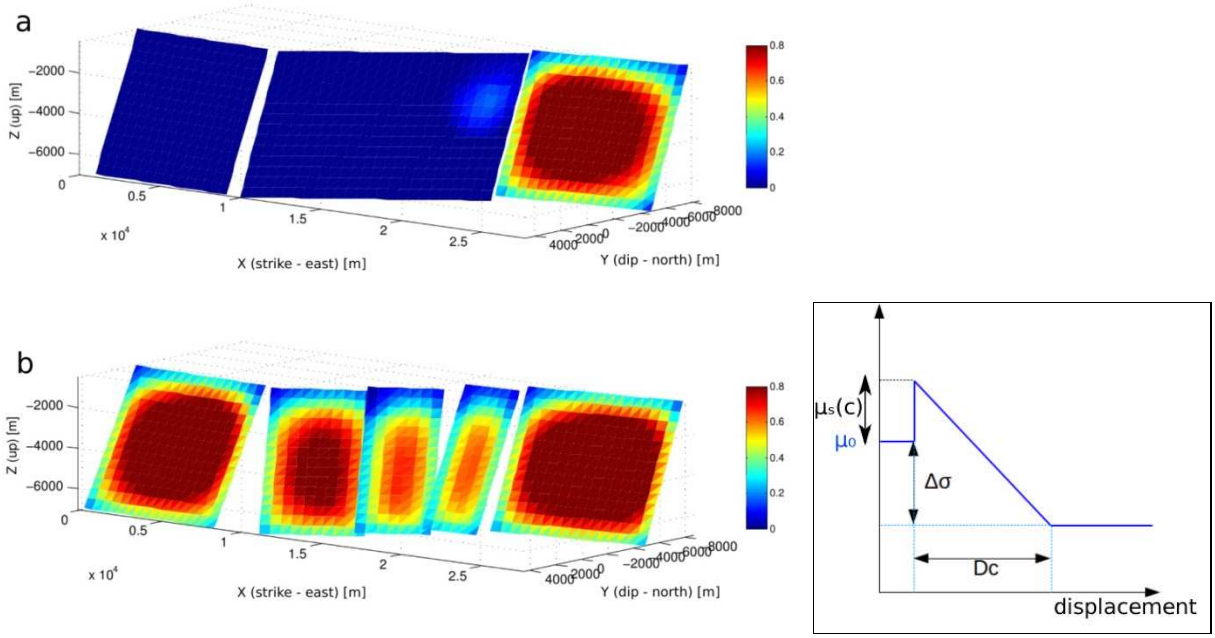

Figure 2. Left: Final slip obtained for two simulations, viewed from the North. a) For a simple geometry, an example of a rupture that stays on the first fault. Dc=0.3m, Mw=6.03 b) For a complex fault geometry, an example of a rupture that propagates on all the faults. Dc=0.1m, Mw=6.35. Right inset: Friction law used in the simulations. c indicates the position in the seismic cycle.

REFERENCES

Boiselet A (2014) Cycle sismique et aléa sismique d'un réseau de failles actives : le cas du rift de Corinthe (Grèce), Ph.D. Thesis, École Normale Supérieure, Paris, France

Hok S and Fukuyama E (2011) "A new BIEM for rupture dynamics in half-space and its application to the 2008 Iwate-Miyagi Nairiku earthquake", *Geophys. J. Int.*, 184:301–324, doi:10.1111/j.1365-246X.2010.04835.x, 11 January 2011

Leonard M (2010) "Earthquake Fault Scaling: Self-Consistent Relating of Rupture Length, Width, Average Displacement, and Moment Release", *Bull. Seismol. Soc. Am.*, 100:1971-1988; doi:10.1785/0120090189

Pacchiani, F. and Lyon-Caen, H. (2010) "Geometry and spatio-temporal evolution of the 2001 Agios Ioanis earthquake swarm (Corinth Rift, Greece)" *Geophys. J. Int.*, 180: 59–72, doi:10.1111/j.1365-246X.2009.04409.x